ARID ZONE JOURNAL OF ENGINEERING, TECHNOLOGY & ENVIRONMENT
AZOJETE March 2024. Vol. 20(1):25-44
Published by the Faculty of Engineering, University of Maiduguri, Maiduguri, Nigeria.
Print ISSN: 1596-2490, Electronic ISSN: 2545-5818
www.azojete.com.ng

EFFECT OF DIELECTRIC PROPERTIES OF BUILDING STRUCTURAL MATERIALS ON ATTENUATION OF MICROWAVE SIGNALS IN URBAN AREAS OF NIGERIA

E. Nwaokolo and A. Gbenga-Ilori*

Department of Electrical and Electronics Engineering, University of Lagos, Akoka, Lagos, Nigeria

**Corresponding author's email address: gbengailori@unilag.edu.ng*

ARTICLE INFORMATION

Submitted 18 Sept., 2023
Revised 15 December, 2023
Accepted 3 January, 2024

Keywords:
Attenuation
Reflection test
Building loss
Propagation
Dielectric Properties

ABSTRACT

Dielectric properties determine how buildings attenuate communication signals. It is therefore an important factor in the propagation of signals. While building loss is an important parameter in link planning, it is often poorly characterized, and the data relating to the effect of building materials on propagation is either unavailable or poorly represented. In this paper, scattering parameters of typical urban buildings in Nigeria are measured to determine signal penetration loss for the frequency range of 800MHz to 3.2GHz. Building materials tested include reinforced concrete slabs, hollow sandcrete blocks, and prefabricated reinforced concrete slabs. The finishing of these materials ranged from burn bricks, rough paint, smooth paint, smooth wall tiles, smooth glassy tiles, to hardwood. The measurements were carried out using the oblique free-space measurement method. The dielectric properties of tested building materials were derived using the new non-iterative conversion method. Model equations that can predict scattering parameters and dielectric properties of a building given the test frequency and thickness of the building were also derived. Comparative analysis of the derived model with actual measurements showed an RMSE value ranging from 0.0192 to 0.2188. Results showed that the frequency of propagation, the thickness of the material under test (building wall), and building finishing affect the dielectric properties and contribute to the signal attenuation experienced in buildings. It was also seen that concrete structures had higher permittivity values hence they had difficulty with microwave signal penetration. Sandcrete blocks are therefore recommended for building walls in urban areas.

1.0 Introduction

Microwave communication is ubiquitous in our everyday lives. It is the backbone for mobile communication, Wi-Fi connectivity, and the Internet of Things (IoT) (Chen *et al*., 2023). Good mobile communication service is dependent on numerous factors including the type of building material, path loss, and interference (Huaman *et al*., 2020; Oladimeji *et al*., 2022; Gómez-Pérez *et al*., 2017; Akobundu and Gbenga-Ilori, 2019). In deploying mobile communication networks in Nigeria, telecommunication companies rely on available data on signal path loss within the vicinity of deployment. In many cases, losses due to buildings are neglected. Though many communication devices are mobile and can be used outdoors, with the advent of IoT, there is an increasing number of communication devices used indoors hence the importance of capturing factors that lead to building losses in communication networks.

A few researchers have considered the impact of buildings on different communication systems. In the work done by Ferreira *et al.* (2017), the authors showed that the materials and dimensions used for building walls can result in the attenuation of microwave signals in radio wave communication. The authors analyzed building materials commonly used in southern Europe. In the work of Zhekov *et al.* (2018), authors studied the loss introduced into radio wave communication by multiple building structures like brick, cavity and solid concrete block, and plasterboard walls; tile and slate roofs; and ten types of modern windows.

The UK Office of Communications, in Rudd *et al.* (2014), studied the impact of increased use of energy-efficient construction practices on building entry loss in communication systems. This study measured the building losses of several properties with a range of different construction materials in the UK, including foil-backed plasterboard and metallized double glazing. Asp *et al.* (2014) examined increased levels of outdoor-indoor attenuation in modern energy-efficient buildings and their impact on mobile cellular networks. Comparative studies of attenuation from such buildings and older buildings were done. The paper also evaluated the use of a dedicated aperture installed in building materials for achieving increased indoor signal coverage.

In reducing the impact of building materials on signal loss in communications systems, authors have considered different solutions. Zhang and Lim (2020) used the Uniform Theory of Diffraction (UTD) where buildings are considered to be flat-surfaced and the ray tracing method was utilized to include diffraction effects on buildings. Ng *et al.* (2022) presented an empirical analysis of the EM wave propagation through composite building materials. The study proposed the use of composite building materials enhanced with different volumetric fractions of iron (III) oxide (Fe2O3) inclusions as a reddish-brown colouring admixture in modern-day concrete, as a means of improving signal penetration in buildings. In most of the literature reviewed, empirical analyses were done on foreign buildings and there is a need to test local Nigerian building materials to have accurate data on the level of attenuation. Danladi *et al.* (2015) investigated GSM signal strength variation in and around mud buildings with rusted corrugated iron sheet roof materials mostly used in the rural areas of Nigeria. Their results showed that the indoor RSS was lower than that of the outdoor consequently contributing to the attenuation of GSM signals. Elechi *et al.* (2018) and Elechi and Otasowie (2015) took measurements of GSM signal strength in buildings made of mud, sandcrete, and alucoboard to determine the signal penetration loss. The measurement results indicated that the building with alucoboard wall cladding had the maximum signal penetration loss, while the sandcrete buildings with unrusted corrugated iron sheet roofs had the minimum signal penetration loss.

In this paper, authors considered reinforced concrete slabs, hollow sandcrete blocks, and prefabricated reinforced concrete slabs materials commonly used in buildings located in urban areas of Nigeria. The finishing of these materials ranged from burn bricks, rough paint, smooth paint, smooth wall tiles, smooth glassy tiles, and hardwood. The goal was to conduct a reflection test which can be used to determine the scattering parameters (S-parameters) of buildings in the microwave frequency range of 800MHz to 3.2GHz and use these results to compute the dielectric properties of the building materials tested in order to quantify the building losses experienced due to the attenuation of communication signals.

Corresponding author's e-mail address: gbengailori@unilag.edu.ng

1. Materials and Method

This work aimed to determine the dielectric properties of typical buildings in urban areas of Nigeria and use these parameters to estimate microwave signal attenuation losses from these buildings. To achieve this, reflection test measurements were first conducted to derive the S-parameters using the Free Space Method (FSM), and the data obtained was used to compute the dielectric properties and attenuation losses of the buildings considered, and develop a predictive model using machine learning. The location of the FSM test was the main campus of the University of Lagos, Lagos, Nigeria, as the area provided access to several building materials commonly used in urban areas in the country.

1.1 Materials

The materials used for the FSM measurement set-up were mainly the vector network analyzer (VNA), antennas, and transmission line as shown in Figure 1. The transmit and receive antennas had to be in far field of each other and the material under test (MUT). The space between these two antennas can be considered as a two-port network whose behavior is characterized by S-parameters which are used to extract the dielectric properties of buildings.

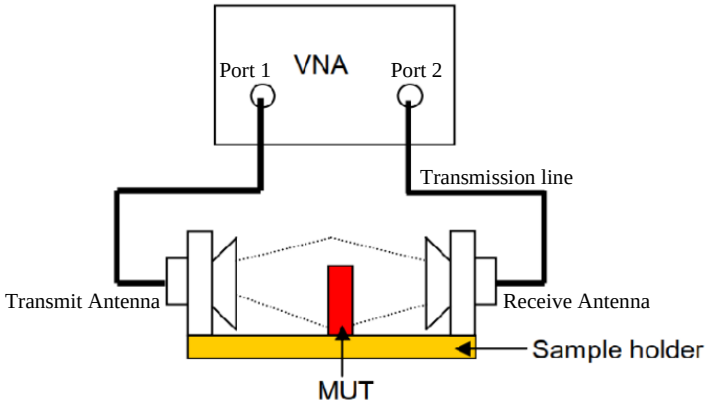

Figure 1: FSM Measurement Set-Up

The MUT tested were selected by examining the buildings to find out typical walls that satisfy the following requirements:

1) MUT contains the same construction material throughout the test plane,
2) distance between the wall and the closest obstacle put the test antennas in far field of the MUT, and
3) MUT has a completely flat wall surface, with no curves or undulations.

The building material under test and for which the measurements were done have dielectric properties. The buildings used were categorized based on age and composite material for erecting the building. For reinforced concrete structures, a structure of 50 years post-completion is considered old but for sandcrete hollow-block structure, a 35-year post-completion structure is considered old according to the Nigerian building code (NBC, 2006). The major building materials used for the structures on the campus of the University of Lagos are reinforced concrete slabs and hollow sandcrete blocks.

Corresponding author's e-mail address: gbengailori@unilag.edu.ng

1.2 Free Space Method (FSM) Measurement

The free space method (FSM) (Sivakumar *et al*., 2022) was used to carry out the reflection tests used to determine the S-parameters. The type of FSM used was the oblique angle system in which both transmitting and receiving antennas were at oblique angles to the measuring plane (Shi *et al*., 2019). The FSM method is most suitable when the MUT has a high temperature, cannot be destroyed under test, has a large flat solid plane, and is large enough to contain the entire beam width of the antenna. In the oblique incidence method, the propagating antenna and receiving antenna are both on the same plane, equidistant from the MUT, and are inclined to the MUT at an oblique angle. For this measurement, the wave emanating from the transmit antenna was incident on the MUT and reflected to the receiving antenna which was inclined at an angle equal to that of the transmit antenna and was equidistant from the centre of the MUT as was the transmit antenna. Using this method, the scattering parameters, forward reflection coefficient (S_{11}) and forward transmission coefficient (S_{21}), were obtained after testing each MUT considered. Figure 2 describes the step used for the FSM test.

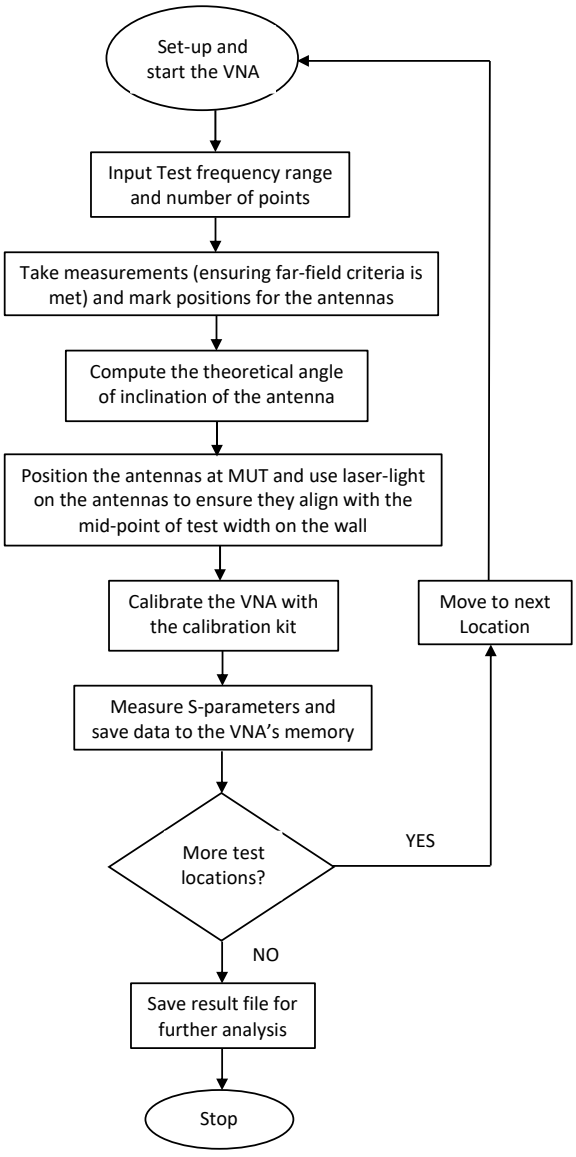

Figure 2: FSM Test and Measurement Steps

The far-field distance between the transmit and receive antennas is determined using Equation (1) (Guo *et al*., 2019):

$$d > \frac{2D^2 f}{C} \qquad (1)$$

where d is the distance between the antenna and MUT in metres, D represents the largest dimension of the antenna plane perpendicular to the direction of radiated waves in metres, C is the speed of light which is $3.0 \times 10^8\ m/s$, and f is the test frequency used for the measurement which was between $800\ MHz$ and $3.2\ GHz$.

Given that the dimension of the antenna D used in this work was $287.4\ mm$, the far-field distance *d* was computed for the $800\ MHz$ and $3.2\ GHz$ frequencies as shown in Equations (2) and (3) respectively:

$d > 0.4405\ m,$ (800 Mhz) (2)

$d > 1.7621\ m,$ (3.2 Ghz) (3)

The antennas were mounted on a moveable wooden pole and positioned perpendicular to the base. The base was fabricated with a knife-edge ending to allow measurements at an angular inclination of the antennas. As stated earlier, the materials under test (MUT) were either reinforced concrete or sandcrete hollow blocks. In total, eighteen (18) locations were used in ten (10) buildings for our measurements and these buildings were labelled B1 to B10. The building tests were also conducted indoors and outdoors.

Five buildings made out of sandcrete hollow blocks were used as MUT and tested in nine (9) locations consisting of indoor and outdoor. The buildings were labelled B3 (point 1) and (point 2), B4, B7, B8, and B9. The average age of the sandcrete block buildings tested was 11 years old and therefore classified as new buildings according to the Nigerian building code (NBC, 2006). Two outdoor tests were carried out on building B3. No indoor tests were carried out because no suitable MUT was found for the test. The MUT at B3 Point 1 (Pt. 1) was a smooth painted wall while the MUT at B3 Point 2 (Pt. 2) had smooth wall tiles as the finishing. Two tests were carried out on building B4, and they were done both indoors and outdoors. The building had a smooth-painted wall finish. One outdoor test was carried out on building B7. The building had a smooth-painted wall finish. Two tests were carried out on building B8, conducted both indoors and outdoors. The outdoor wall of the building used as the MUT had burnt-brick tiles as the finishing while the indoor MUT had a smooth-painted wall finishing. Two tests were carried out both indoor and outdoor on building B9. The building had a smooth-painted wall finish.

Five buildings made out of reinforced concrete structures were tested in nine (9) locations. The buildings were labelled B1, B2, B5, B6, and B10. The average age of the buildings tested was forty-nine (49) years old which classifies all of them as old buildings according to the Nigerian building code (NBC, 2006). Building B1 test location had a burned brick finish on it. The finishing material of building B2 was rough-painted walls. Building B5 had smooth glassy wall tiles finish while building B6 had a rough wall paint finish for both indoor and outdoor. Building B10 had a smooth-painted wall finish.

The scattering parameters S_{11} and S_{21} determined from the process described in Figure 2 were then used to determine the dielectric properties of the MUT by subjecting the test result to the new non-iterative algorithm (Luukkonen *et al*., 2011). This algorithm relies on a system of equations to compute the permeability and permittivity. These dielectric parameters were used

Corresponding author's e-mail address: gbengailori@unilag.edu.ng

to determine the level to which the MUT attenuates communication signals. The frequency used for the measurement test was in the range of 800MHz and 3.2GHz, since most telecommunication 3G, 4G, and Wi-Fi frequency signals are within this band.

2.3 Computation of Dielectric Parameters of Buildings

The goal was to use the measured S_{11} and S_{21} parameters to determine the permittivity and permeability of the buildings using the new non-iterative method (Kharkovsky, 2002). The parameters and steps needed for the new non-iterative method are shown in Figure 3.

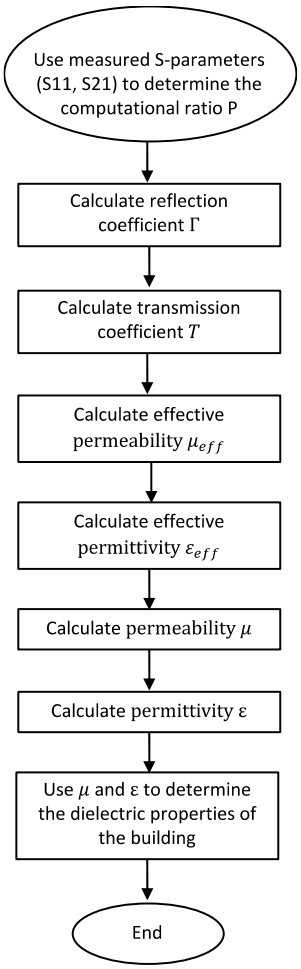

Figure 3: Steps for the New non-iterative method (Kharkovsky, 2002)

Equations (4) to (12) are the system of equations that make up the new non-iterative conversion model to convert our measured S parameters into dielectric properties of the MUT. Given the S parameters, a computational ratio P (Kharkovsky, 2002) can be defined to simplify the process:

$$P = \frac{S_{11}^2 - S_{21}^2 + 1}{2S_{11}}. \tag{4}$$

The reflection coefficient *Γ* is:

$$\Gamma = P \pm \sqrt{(P^2 - 1)}, \tag{5}$$

while the transmission coefficient T is:

$$T = \frac{S_{11} + S_{21} - \Gamma}{1 - \Gamma(S_{11} + S_{21})}. \tag{6}$$

Corresponding author's e-mail address: gbengailori@unilag.edu.ng

A parameter Λ can also be defined in terms of the transmission coefficient such that:

$$\frac{1}{\Lambda^2} := -\left(\frac{1}{2\pi d'} ln\left(\frac{1}{T}\right)\right)^2 \tag{7}$$

where d' is the thickness of the material being measured (Kharkovsky, 2002). The wavelength of propagation in an empty cell λ_{og} in *metres* is:

$$\lambda_{og} = \frac{1}{\sqrt{\frac{1}{\lambda_0^2} - \frac{1}{\lambda_c^2}}} \tag{8}$$

where λ_0 is the free-space wavelength in *metres* and λ_c is the cut-off wavelength in *metres.*

The effective permeability of the material (H/m) is given as (Kharkovsky, 2002):

$$\mu_{eff} = \frac{\lambda_{og}}{\Lambda}\left(\frac{1+\Gamma}{1-\Gamma}\right), \tag{9}$$

and the effective permittivity of the material (F/m) is given as:

$$\varepsilon_{eff} = \frac{\lambda_{og}}{\Lambda}\left(\frac{1-\Gamma}{1+\Gamma}\right). \tag{10}$$

The permeability of the material (H/m) is (Kharkovsky, 2002):

$$\mu = \mu_{eff} = \frac{\lambda_{og}}{\Lambda}\left(\frac{1+\Gamma}{1-\Gamma}\right), \tag{11}$$

while the permittivity of the material (F/m) is given as:

$$\varepsilon = \left(\left(1 - \frac{\lambda_0^2}{\lambda_c^2}\right) \times \varepsilon_{eff}\right) + \left(\left(\frac{\lambda_0^2}{\lambda_c^2}\right) \div \mu_{eff}\right). \tag{12}$$

MATLAB was used for the computation of the metrics used to determine the permittivity (ε), and permeability (μ) of the buildings measured.

The attenuation constant for each test location was later computed from the dielectric parameters using Equation (13), (Pozar, 2011). The attenuation constant shows the degree to which a signal degrades as it traverses the building.

$$\alpha = \omega \sqrt{\frac{\mu\varepsilon}{2}\left\{\sqrt{1 + \frac{\sigma^2}{\omega^2\mu^2}} - 1\right\}} \tag{13}$$

where α is the attenuation constant of the wave in Nepers/metre as it propagates through a medium, σ is the conductivity value of the MUT in *S/m*, and ω is the angular frequency of the EM wave in *rads/s*.

The loss tangent δ is given in Equation (14):

$$\tan\delta = \frac{\varepsilon^{"}}{\varepsilon'} = \frac{\sigma}{\omega\varepsilon'} \tag{14}$$

where $\varepsilon^{"}$ is the imaginary part of the permittivity which connotes how much energy radiated is dissipated by the material while ε' is the real part of the permittivity which connotes how much electric energy is absorbed or stored in the material. By comparing Equations (13) and (14), the α in Nepers/m could be re-written as:

$$\alpha = \omega\sqrt{\frac{\mu\varepsilon'}{2}\left\{\sqrt{1+\left(\frac{\varepsilon^{"}}{\mu}\right)^{2}}-1\right\}} \tag{15}$$

The attenuation constant can also be written in *dB/m* which is more relatable by using the conversion metric shown in Equation (16):

$$\alpha\ (dB/m) = 8.86 \times \alpha\ (Nepers/m). \tag{16}$$

The attenuation factor in this work was measured for 1800MHz and 2600 MHz as these were the frequencies used by network operators in all locations tested.

2.4 Predictive Model

A predictive model was developed in this paper with machine learning using linear regression techniques to achieve two main objectives: To

- establish a statistical relationship between the input and output variables to obtain a general characteristic equation with minimal error values using measurements taken, and
- predict new observations with minimal errors using the equation set that makes up the model.

The model was developed using Python to simulate the linear regression techniques shown in Equation (17):

$$z_j = \beta_0 + \beta_1\omega_j + \beta_2\eta_j + e_j \tag{17}$$

where z_j is the dependent variable, ω and η are the independent variables, β_0 is the constant or intercept, β_1 is the slope or coefficient of ω, β_2 is the slope or coefficient of η, e is the error term, and *j* is numbers 1,2,3,4…n.

The Python libraries imported to develop the model include *numpy*, *cmath*, *pandas*, and *matplotlib*. Equation (18) shows that the dependent variable has both the real and imaginary parts:

$$z_j = x_j + iy_j \tag{18}$$

where *x* and *y* are the values of the complex numbers of the dependent variable z_j. Therefore

$$\beta_0 = \gamma_0 + i\delta_0 \quad \beta_1 = \gamma_1 + i\delta_1 \quad \beta_2 = \gamma_2 + i\delta_2 \tag{19}$$

Corresponding author's e-mail address: gbengailori@unilag.edu.ng

To minimize the errors in Equation (17), the minimization problem in Equation (20) is solved:

$$\underset{\beta_0,\beta_1,\beta_2}{arg\,min} \sum_{j=1}^{n} \left\| z_j - \left(\hat{\beta}_o + \hat{\beta}_1\omega_j + \beta_2\eta_j\right)\right\|^2$$

$$= \underset{\beta_0,\beta_1,\beta_2}{arg\,min} \sum_{j=1}^{n} \left(\overline{z_j} - \left(\overline{\hat{\beta}_o} + \overline{\hat{\beta}_1}\omega_j + \beta_2\eta_j\right)\right)\left(z_j - \left(\beta_0 + \beta_1\omega_j + \beta_2\eta_j\right)\right) \quad (20)$$

Equation (20) is principally used to perform the regression on the model using the uploaded dataset. Comparing Equations (17) and (20), the value of error can be minimized and $\beta_0,\ \beta_1,\ \beta_2$ can be obtained as they are the parameters for which the error values are minimum.

$$\|z\|^2 = z\bar{z} \quad (21)$$

$$\hat{\beta} = (X^*X)^{-1}X^*z \quad (22)$$

$$X^* = \bar{X}^T \quad (23)$$

The dataset was made up of mainly complex numbers. In organizing the data, the dataset was segmented into four parts: data from reinforced concrete blocks (indoor), data from reinforced concrete blocks (outdoor), data from sandcrete blocks (indoor), and data from sandcrete blocks (outdoor). The input variables were the thickness of MUT, building type (concrete or sandcrete), and measurement environment (indoor or outdoor). The output variables were S_{11}, S_{21}, μ, and ε. The prepared model was trained using the dataset and β-values were computed to produce a general equation that can be used to make predictions. A general equation was obtained from the model which was used to accurately predict S_{11}, S_{21}, μ, and ε when input variables are provided.

In preparing the model, the input parameters selected are the test frequency and the thickness of the wall or MUT. Hence Equation (17) can be rewritten as Equation (24):

$$z_j = \beta_0 + \beta_1 freq_j + \beta_2 thickness_j + e_j \quad (24)$$

By training the model, the best values for β_0, β_1, β_2, and e were obtained to give a general equation for making output predictions. Sixteen sets of values β_0, β_1, β_2, and the error e were obtained and were used to predict the corresponding output value:

$$\hat{y} = [\beta_0\,\beta_1\beta_2]^T[1\ \omega\ \eta] \quad (25)$$

where ω represents the test frequency and η represents the thickness of the MUT. The system of 16 equations constitutes the model and can be used to predict the S_{11}, S_{21}, μ, and ε values of a MUT which could be made of concrete or sandcrete blocks, and could be an outdoor or indoor MUT.

To quantify the deviation of the predicted value from the actual measured value, the root mean square error (RMSE) computation was done using Equation (26). RMSE values were computed for each of the 16 characteristic equations and this produced 16-RMSE values.

Corresponding author's e-mail address: gbengailori@unilag.edu.ng

$$RMSE = \frac{\sqrt{\sum_{i=1}^{N} |z_i|^2}}{N} \tag{26}$$

In testing the suitability of the model, the RMSE values were normalized using Equation (27).

$$normalized\ RMSE = \frac{RMSE}{\max value - \min value} \tag{27}$$

where the *max value* is the highest value of the dataset, and the *min value* is the lowest value of the dataset. Some of the *max value and min value* used for RMSE normalization were complex numbers, hence Equation (28) was used to obtain the absolute values.

$$z = x + yi \tag{28}$$

$$|z| = \sqrt{(x + yi)(x - yi)} \tag{29}$$

When data is normalized it ranges from 0 to 1. The closer the normalized data is to zero, the better the model is at making accurate predictions.

3. Results and Discussion

This section presents the results and analysis of the models used. As stated earlier, the materials under test (MUT) were either reinforced concrete or sandcrete hollow blocks. In total, eighteen (18) locations were used in our measurements and these MUTs were labelled B1 to B10. Figures 4, 5, 6 and 7 show the dielectric properties measured outdoors for all the buildings while Figures 8, 9, 10 and 11 show the dielectric properties measured indoors for all the buildings.

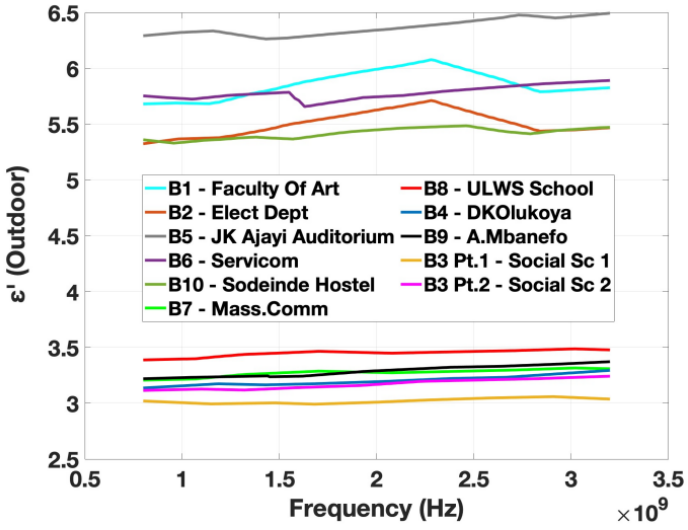

Figure 4: Dielectric plots for Buildings - Outdoor Permittivity Real (_′)

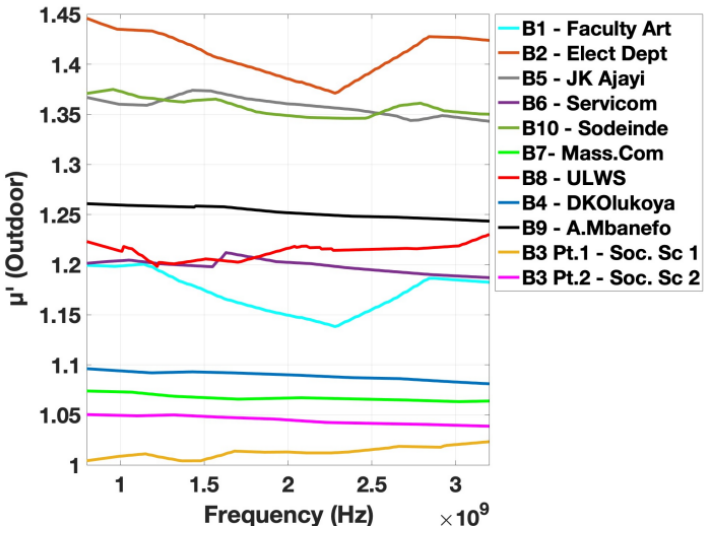

Figure 5: Dielectric plots for Buildings - Outdoor Permeability Real (_′)

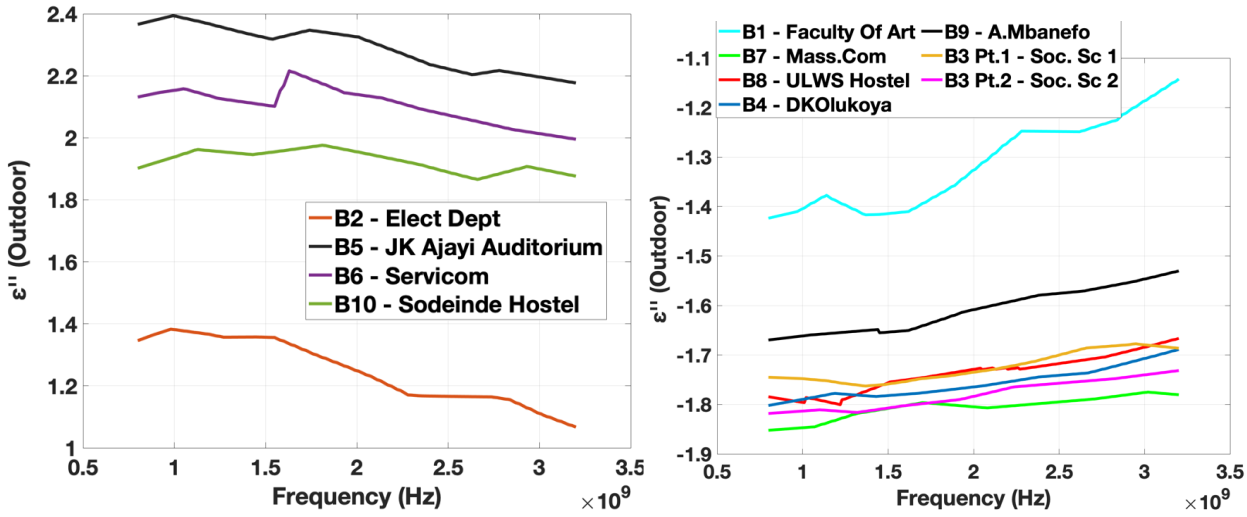

Figure 6: Dielectric plots for Buildings – Outdoor Permittivity Img (_′′)

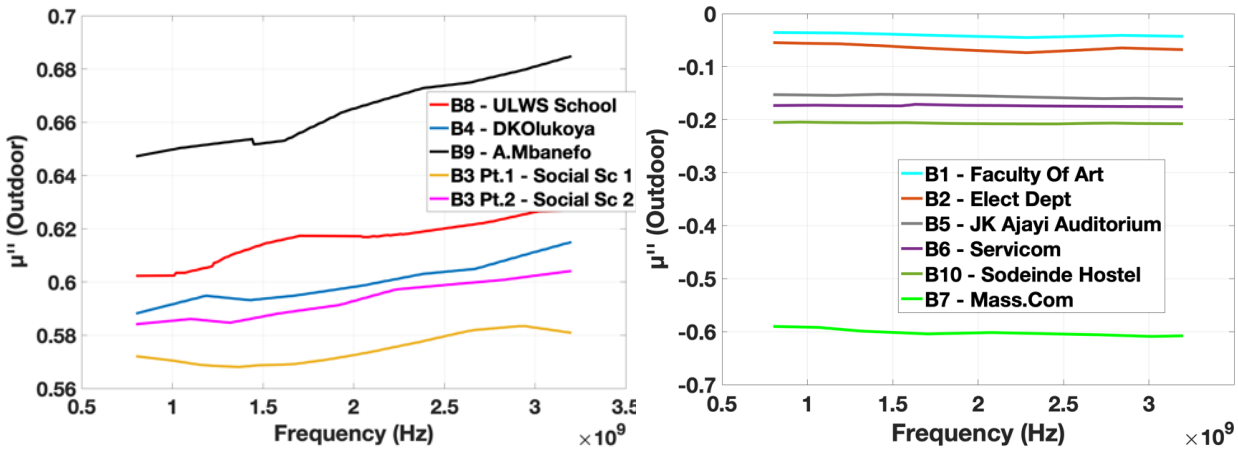

Figure 7: Dielectric plots for Buildings – Outdoor Permeability Img (_′′)

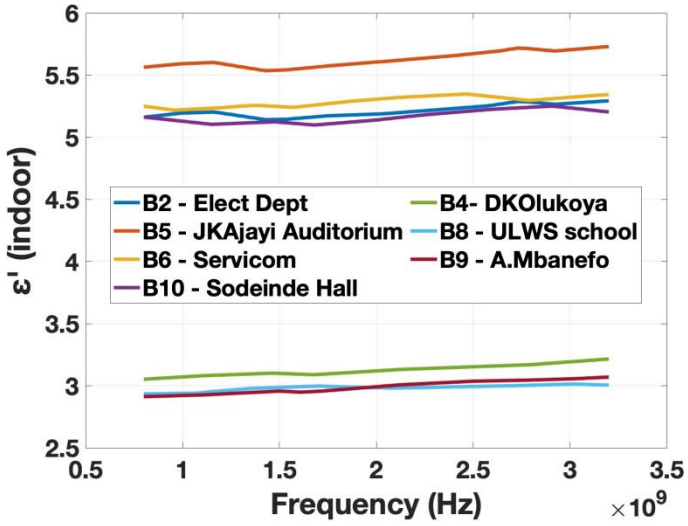

Figure 8: Dielectric plots for Buildings – Indoor Permittivity Real (ε')

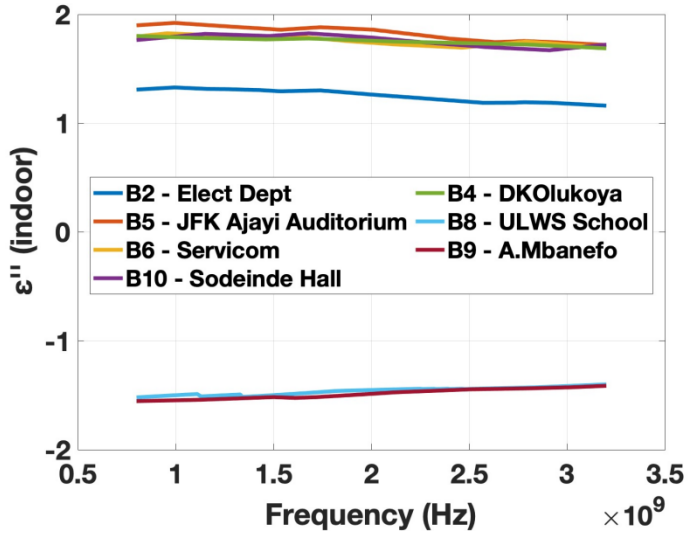

Figure 9: Dielectric plots for Buildings - Indoor Permittivity Img (ε'')

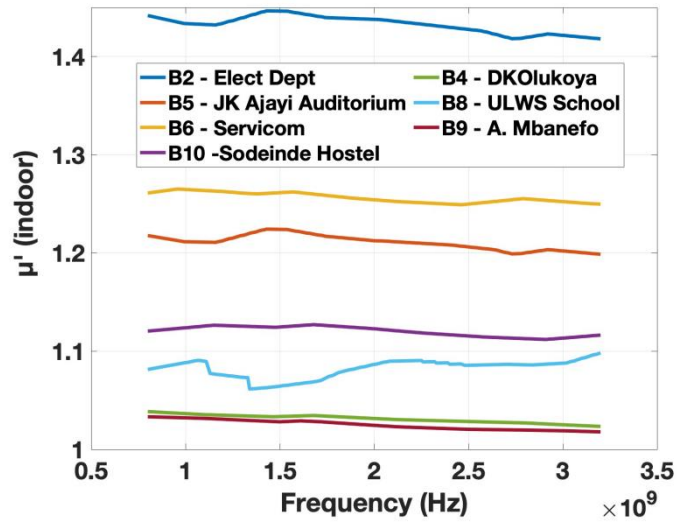

Figure 10: Dielectric plots for Buildings - Indoor Permeability Real (μ')

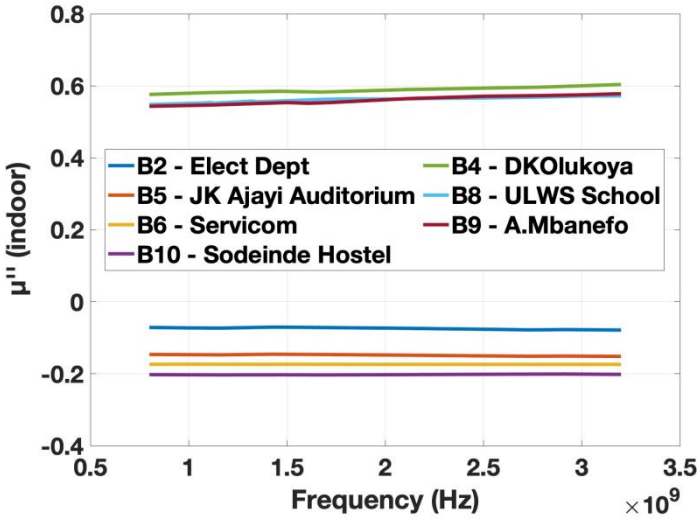

Figure 11: Dielectric plots for Buildings - Indoor Permeability Img (μ'')

3.1 Results for Sandcrete Block Structures

Results for the five buildings made out of sandcrete hollow blocks tested in nine (9) locations are presented in this section. The buildings include B3 (point 1), B3 (point 2), B4, B7, B8, and B9.

3.1.1 Building B3 -Point 1 and Point 2 (Outdoor)

Results of the dielectric properties for building B3 show a difference between the permittivity value range of 3.0245 – 3.0377 for building B3 (Pt. 1) and the permittivity value range of 3.1153 – 3.2428 for building B3 (Pt. 2) as shown in Figure 4. This was due to slight variations in the thickness of MUT and the finishing of the buildings. The permittivity range for B3 (Pt. 1) was between 3.0196 to 3.0377 and for B3 (Pt. 2) between 3.11535 to 3.2428 as shown in Figure 4, while permeability values for B3 (Pt. 1) range is 1.0042 - 1.0231 and for B3 (Pt. 2) is 1.0502 - 1.0387 as shown in Figure 5. The loss tangents are shown in Figures 6 and 7. With these permittivity and permeability results, the attenuation constants related to the use of microwave signal reception within this building were quantified in dB/m for 1800 MHz and 2600MHz frequencies as shown in Table 1. It can be deduced from Table 1 that higher propagation frequencies experienced higher attenuation losses given the same MUT. In building B3, microwave signals from telecommunication base transceiver stations (BTS) experienced attenuation losses of between 3.2887 to 4.78 dB/m depending on the propagation frequency used.

Table 1: Computed Building Attenuation losses at B3

Test Location	Propagation Frequency (MHz)	Permittivity	Permeability	Attenuation Constant *(dB/m)*
B3	1800	3.0032 -1.7408i	1.0128	3.2887
Point1	2600	3.0500- 1.6857i	1.0186	4.5279
B3	1800	3.1575- 1.7912i	1.0460	3.4142
Point2	2600	3.2138- 1.7526i	1.0410	4.7800

Corresponding author's e-mail address: gbengailori@unilag.edu.ng

3.1.2 Building B4 (Outdoor and Indoor)

Results for building B4 show that the outdoor permittivity value was between 3.1371 and 3.2711 as shown in Figure 4, while the indoor permittivity value had a range of 3.0522 to 3.1921 as shown in Figure 8. The main factor for the difference was the variation in the thickness of the outdoor and indoor walls. The attenuation constant which is an indication of the losses associated with the microwave communication in the building was computed and results are shown in Table 2. In this building, microwave signals from telecommunication base transceiver stations (BTS) experienced attenuation losses of between 3.3176 and 4.7056 dB/m depending on the propagation frequency used.

Table 2: Computed Attenuation losses at B4

Test Location	Propagation Frequency (MHz)	Permittivity	Permeability	Attenuation Constant *(dB/m)*
Outdoor	1800	3.1868 - 1.7691i	1.0907	3.3176
	2600	3.2327- 1.7366i	1.0862	4.6504
Indoor	1800	3.1085 - 1.7655i	1.0325	3.3608
	2600	3.1618 - 1.7282i	1.0276	4.7056

3.1.3 Building B7 (Outdoor)

One outdoor test was carried out on building B7. The permittivity value range for building B7 was between 3.2074 and 3.3093 as shown in Figure 4. It was deduced that permittivity increases with frequency. Table 3 shows that attenuation losses experienced in this building ranged between 3.4664 and 4.8888 *dB/m* depending on the propagation frequency used. Figures 4 to 7 show the dielectric properties for measurements taken outdoors.

Table 3: Computed Attenuation losses at B7

Test Location	Propagation Frequency (MHz)	Permittivity	Permeability	Attenuation Constant *(dB/m)*
Outdoor	1800	3.2808- 1.8014i	1.0664	3.4664
	2600	3.2960- 1.7903i	1.0650	4.8888

3.1.4 Building B8 (Outdoor and Indoor)

Two tests were carried out on this building, conducted both indoors and outdoors. It was noticed that the indoor test carried out produced the lowest measured permittivity value of 2.9344 as shown in Figure 8. This was a result of the finishing and also the thickness of the wall which was also the smallest value measured at 0.1922 metres. The outdoor permittivity value ranged from 3.3883 to 3.4784 as shown in Figure 4, while the indoor permittivity value ranged from 2.9344 to 3.0051 as shown in Figure 8. The attenuation loss value range was between 2.6570 and 4.4824 dB/m as shown in Table 4.

Table 4: Computed Attenuation losses at B8

Test Location	Propagation Frequency (MHz)	Permittivity	Permeability	Attenuation Constant *(dB/m)*
Indoor	1800	2.9891 - 1.4569i	1.0817	2.6570
	2600	2.9990 - 1.4346i	1.0864	3.6999
Outdoor	1800	3.4573 - 1.7354i	1.2100	3.2170

Corresponding author's e-mail address: gbengailori@unilag.edu.ng

	2600	3.4700 - 1.7094i	1.2160	4.4824

3.1.5 Building B9 (Outdoor and Indoor)

Results from tests on building B9 showed a difference between the outdoor permittivity value with a range of 3.1371 to 3.2711 as shown in Figure 4 and the indoor permittivity value with a range of 3.0522 to 3.1921 as shown in Figure 8. This was mainly due to variations in the thickness of the outdoor and indoor walls. The attenuation loss value range was between 2.8019 and 3.9828 dB/m as shown in Table 5.

Table 5: Computed Attenuation losses at B9

Test Location	Propagation Frequency (MHz)	Permittivity	Permeability	Attenuation Constant *(dB/m)*
Indoor	1800	3.2785 - 1.6196i	1.2533	2.8738
	2600	3.3326 - 1.5697i	1.2473	3.9828
Outdoor	1800	2.9776 - 1.4991i	1.0259	2.8019
	2600	3.0416 - 1.4408i	1.0200	3.8621

From the results shown in Tables 1 to 5, it can be concluded that the highest permittivity value of 3.47835 was recorded during the outdoor testing of Building B8. This value was recorded as a result of two main factors; the thickness of the wall and the burn-brick tiles finishing which added to the measured permittivity value. The values of complex permittivity computed agree with published values (Vilovic et al., 2008). There were some scenarios in which the computed values exceeded the known published values, and this was due to the difference in thickness of MUT encountered in our testing over those used in published works, as well as the difference in finishing used in the buildings tested. The values of loss tangent computed and shown in Figures 6,7, 10 and 11 agree with that of published scientific works. The loss tangent values were less than 1, and in a few scenarios, the values were close to 1. From computed dielectric values and attenuation constants, the sandcrete hollow block MUTs can be considered lossy dielectrics and will offer some opposition to communication signals due to the high level of attenuation. The range of the attenuation loss recorded was between 2.6570 dB and 4.888 dB depending on the microwave frequency.

3.2 Results for Concrete Structures

Presentation of results for the five buildings made out of reinforced concrete structures are presented in this section. Nine (9) locations were tested indoors and outdoors and these buildings were labelled B1, B2, B5, B6, and B10.

3.2.1 Building B1 (Outdoor)

Building B1 had only one test done outdoors. The permittivity value of the MUT was determined to be between 5.682 and 5.8247 as shown in Figure 4. The range of the attenuation loss was between 4.6912 and 6.4946 dB/m as shown in Table 6. This value connotes that communication signals would experience high losses as they penetrate the building walls. The thickness of the MUT measured was 0.2465 m, a good part of the perimeter walls of the

Corresponding author's e-mail address: gbengailori@unilag.edu.ng

building exceeds this value. A higher attenuation level was therefore experienced in some locations of the building.

Table 6: Computed Attenuation losses for B1

Test Location	Propagation Frequency (MHz)	Permittivity	Permeability	Attenuation Constant *(dB/m)*
Outdoor	1800	5.9613 + 1.8575i	1.1249	4.6912
	2600	5.8927 + 1.8447i	1.1455	6.4946

3.2.2 Building B2 (Outdoor and Indoor)

For building B2, the difference between the permittivity value of 5.32511 measured outdoors and the value of 5.16218 measured indoors was not very significant as shown in Figures 4 and 8, and this was a departure from the trend. This resulted due to a slight difference between the thickness of the outdoor wall (0.2535 m) and the thickness of the indoor wall (0.2015 m). Furthermore, the rough-painted walls were the same and therefore presented almost the same test conditions in both scenarios. The attenuation loss value range was between 3.9939 and 6.1939 dB/m as shown in Table 7.

Table 7: Computed Attenuation losses for B2

Test Location	Propagation Frequency (MHz)	Permittivity	Permeability	Attenuation Constant *(dB/m)*
Outdoor	1800	5.5935 + 1.8754i	1.2915	4.2818
	2600	5.5290 + 1.8652i	1.2081	6.1939
Indoor	1800	5.1807 + 1.2801i	1.4387	3.9939
	2600	5.2718+ 1.8878i	1.2219	6.0867

3.2.3 Building B5 (Outdoor and Indoor)

The outdoor wall for building B5 had the thickest wall dimension of 0.2940 m among all the concrete walls measured and it also had a smooth glassy wall tiles finish. These factors combined to make the building produce the highest permittivity value of 6.85039 as shown in Figure 4. The attenuation losses for both indoor and outdoor are shown in Table 8.

Table 8: Computed Attenuation losses for B5

Test Location	Propagation Frequency (MHz)	Permittivity	Permeability	Attenuation Constant *(dB/m)*
Outdoor	1800	6.3265 + 2.3355i	1.3629	5.5204
	2600	6.4588+ 2.2061i	1.3476	7.4969
Indoor	1800	5.5919 + 1.8696i	1.2145	4.4012
	2600	5.7009 + 1.7464i	1.2024	5.9027

Corresponding author's e-mail address: gbengailori@unilag.edu.ng

3.2.4 Building B6 (Outdoor and Indoor)

Building B6 test location had a rough wall paint finish for both indoors and outdoors. The outdoor MUT had a thickness of 0.2828 metres, a slightly higher value than that of B2 which was 0.2535 m. The permittivity value of the test location at a frequency of 800 MHz was 5.7545, a higher value than the 5.3281 obtained in the outdoor testing of building B2 at the same frequency as shown in Figure 4. It was deduced that a slight increase in the thickness of MUT can significantly influence the permittivity values. The attenuation losses computed at different propagation frequencies are shown in Table 9.

Table 9: Computed Attenuation losses for B6

Test Location	Propagation Frequency (MHz)	Permittivity	Permeability	Attenuation Constant *(dB/m)*
Outdoor	1800	5.7266 + 2.1570i	1.2043	5.1603
	2600	5.8366 + 2.0531i	1.1926	7.0503
Indoor	1800	5.2927 + 1.7535i	1.2559	3.9492
	2600	5.3180+ 1.7274i	1.2528	5.5245

3.2.5 Building B10 (Outdoor and Indoor)

Results for building B10 showed a difference between the outdoor permittivity value ranging from 5.3613 to 5.4728 as shown in Figure 4, and the indoor permittivity value ranging from 5.1630 to 5.2041 as shown in Figure 8. This was due to variations in the thickness of the outdoor and indoor walls. The attenuation loss value ranged between 4.2189 and 5.6948 dB/m as shown in Table 10. These values connote that communication signals would experience high losses as they penetrate the building walls.

Table 10. Computed Attenuation losses for B10

Test Location	Propagation Frequency (MHz)	Permittivity	Permeability	Attenuation Constant *(dB/m)*
Outdoor	1800	5.4360 + 1.9682i	1.3505	4.3321
	2600	5.4353 + 1.8661i	1.3584	5.7942
Indoor	1800	5.1249 + 1.8012i	1.1243	4.2189
	2600	5.2308 + 1.6929i	1.1138	5.6948

In summary, the permeability values obtained when testing the concrete buildings ranged from 1.12044 to 1.689166 as shown in Figure 10. Permeability values should be as close as possible to 1, which is the approximate relative permeability of most non-metals. A few of the values obtained were between 1 and 2. This is a drawback of the new non-iterative method used for permittivity and permeability extraction. This method produces better permittivity results but introduces slight errors when computing permeability values. The method was however adopted since accuracy in permittivity values is paramount for this work. From the data obtained, the outdoor measurement of the B5 building yielded the highest permittivity value of 6.85039 due to wall thickness and building finishing. These values showed that a large amount of microwave energy can be absorbed and stored in the walls of the building tested. The values of the computed loss tangent agree with that of the published scientific work of Stavrou et al. (2003). The loss tangent values obtained for reinforced concrete MUTs are significantly lesser

than the values obtained for the sandcrete buildings. It was deduced that the MUTs tested for reinforced concrete have more lossy dielectric properties and will offer more obstruction to communication signals than the sandcrete block buildings from the range of attenuation.

In the above-mentioned buildings, the underlining building material used was reinforced concrete with high permittivity values of up to *6.85039*. This connotes that the walls of the buildings absorb much of the signal. These buildings also have their internal walls made of reinforced concrete and this further attenuates communication signals. The use of repeaters can significantly improve the communication signal indices for these buildings (Fata and Aboulila, 2017). In addition, adopting 5G telecommunication can provide better indoor communication, since it has a more compact base station that can be deployed much closer to the indoor user equipment.

Figures 12 and 13 show plots comparing the predicted S_{21} and ε using the model described in this paper and actual measured values. Analysis of the reliability of this model was carried out under error analysis. For each data set, errors between predicted and measured values were determined using the RMSE. Results show that the least RMSE value was 0.00778376, and this was obtained from the prediction of the S_{21} parameters for indoor sandcrete hollow blocks. The highest RMSE value was 0.218891, and it was obtained from the prediction of the permittivity for an outdoor reinforced concrete slab. To test the suitability of the model, the RMSE values were normalized. The highest normalized value obtained for any wall type was 0.300973105. In general, the values obtained were closer to 0 than to 1, hence indicating that the predictive model was good and reliable.

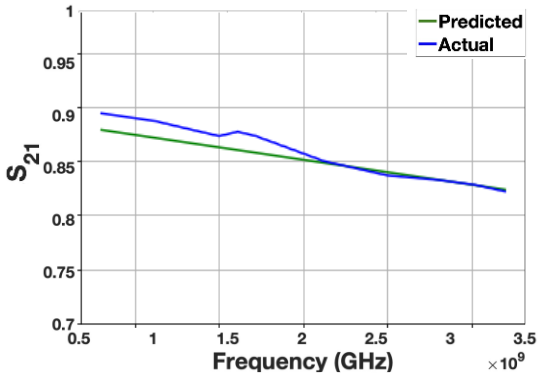

Figure 12: Plot of predicted and actual S_21 versus Frequency

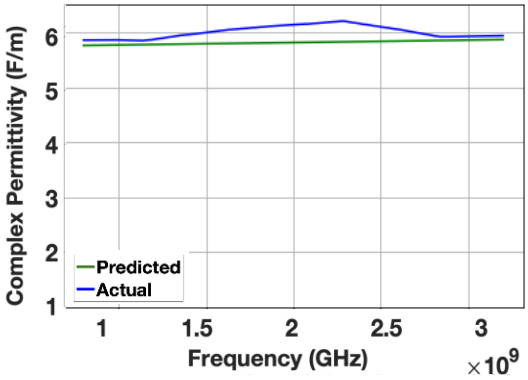

Figure 13: Plot of predicted and actual complex permittivity versus Frequency.

4. Conclusion

The study in this paper was undertaken to determine the microwave signal attenuation factor of common building materials in urban areas of Nigeria. Measurements of the S-parameters were first taken and the data obtained was used to compute the dielectric properties of the buildings after which a predictive model using machine learning was developed. The model was able to predict, with very minimal error, the permittivity, permeability, and S-parameters when known information such as test frequency, and underlining building materials was provided. The model produced a minimum RMSE of 0.007784 when predicting the S_{11} values of indoor walls of sandcrete buildings, while it produced a maximum RMSE value of 0.21889 when predicting the permeability of outdoor concrete walls. Results from this work showed that the frequency, thickness of the MUT (building wall), and building finishing impact the dielectric properties of the buildings. It was also observed that concrete structures produced higher

Corresponding author's e-mail address: gbengailori@unilag.edu.ng

permittivity values hence the MUT shows decreased susceptibility to microwave signal penetration. Though this work was limited to the microwave frequency band up to 3.2 *GHz*, future work can be directed at measuring a wider bandwidth of up to 40 *GHz* so as to accurately determine how the dielectric properties of the buildings would impact 5G communication. It is recommended that the use of sandcrete blocks for building walls should be encouraged as this offers improved dielectric properties and reduced attenuation of microwave signals. Furthermore, when spaces are to be carved out from open areas, especially in buildings made from concrete, effort should be made to use materials with better dielectric properties like plywood, and PVC and reduce the use of materials like aluminium and glass which have higher permittivity values.

References

Akobundu, GC. and Gbenga-Ilori, AO. 2019. GPS Anti-Jamming Technique Using Smart Antenna Systems. Arid Zone Journal of Engineering, Technology and Environment, 15(1): 1-16.

Asp, A., Sydorov, Y., Keskikastari, M., Valkama, M. and Niemela, J. 2014. Impact of modern construction materials on radio signal propagation: Practical measurements and network planning aspects. In 2014 IEEE 79th Vehicular Technology Conference, 18th to 21st May 2014, Seoul, Korea., 79: 1-7.

Chen, W., Lin, X., Lee, J., Toskala, A., Sun, S., Chiasserini, CF. and Liu, L. 2023. 5G-Advanced Toward 6G: Past, Present, and Future. IEEE Journal on Selected Areas in Communications, 41(6): 1592-1619.

Danladi, TA., Ahmed, M. and Nyitamen, DS. 2015. Investigation of building Penetration Loss for GSM Signals into Selected Building Structures in Kaduna. IOSR Journal of Electronics and Communication Engineering, 10(4): 56 - 60.

Elechi, P., Edeko, F. and Egwaile, J. 2018. Relative Permittivity Based Model for GSM Signal Loss in Buildings. Journal of Electrical Engineering, Electronics, Control and Computer Science, 4(2): 19-26.

Elechi, P. and Otasowie, PO. 2015. Determination of GSM signal penetration loss in some selected buildings in Rivers State, Nigeria. Nigerian Journal of Technology, 34(3): 609-615.

Fata, AA. and Aboulila, MM. 2017. In-building solutions using distributed antenna system based on fractal array. In 2017 Progress In Electromagnetics Research Symposium Spring (PIERS), 22nd to 25th May 2017, St. Petersburg, Russia., 984-987.

Ferreira, D., Caldeirinha, RF., Fernandes, TR. and Cuinas, I. 2017. Hollow clay brick wall propagation analysis and modified brick design for enhanced Wi-Fi coverage. IEEE Transactions on Antennas and Propagation, 66(1): 331-339.

Gómez-Pérez, P., Crego-García, M., Cuiñas, I. and Caldeirinha, RF. 2017. Modeling and inferring the attenuation induced by vegetation barriers at 2G/3G/4G cellular bands using Artificial Neural Networks. Measurement, 98: 262-275.

Guo, QY. and Wong, H. 2019. A millimeter-wave Fabry–Pérot cavity antenna using Fresnel zone plate integrated PRS. IEEE Transactions on Antennas and Propagation, 68(1): 564-568.

Corresponding author's e-mail address: gbengailori@unilag.edu.ng

Huaman, JR., Postigo-Malaga, M., Yanyachi, P. and Chilo, J. 2020. Measurements of 3G and 4G signal attenuation in adobe buildings structures. In 2020 IEEE International Instrumentation and Measurement Technology Conference (I2MTC), 30th June 2020, Dubrovnik, Croatia: 1-6.

Kharkovsky, SN., Akay, MF., Hasar, UC. and Atis, CD. 2002. Measurement and monitoring of microwave reflection and transmission properties of cement-based specimens. IEEE Transactions on Instrumentation and Measurement, 51(6): 1210-1218.

Luukkonen, O., Maslovski, SI. and Tretyakov, SA. 2011. A stepwise Nicolson–Ross–Weir based material parameter extraction method. IEEE Antennas and Wireless Propagation Letters, 10: 1295-1298.

NBC, 2006. National Building Code. Fed. Repub. Niger. National Building Code, Ministry of Housing and Urban Development: 1 – 476.

Ng, JP., Sum, YL., Soong, BH., Maier, M. and Monteiro, PJ. 2022. Electromagnetic wave propagation through composite building materials in urban environments at mid-band 5G frequencies. IET Microwaves, Antennas and Propagation, 16(10): 627-638.

Oladimeji, TT., Kumar, P. and Oyie, NO. 2022. Propagation path loss prediction modelling in enclosed environments for 5G networks: A review. Heliyon, 8(11): 1-16.

Pozar, DM. 2011. Microwave engineering. Hoboken, NJ: John Wiley & Sons.

Rudd, R., Craig, K., Ganley, M. and Hartless, R. 2014. Building materials and propagation. Office of Communications (OFCOM) Final Report. London, UK: 2604.

Shi, D., Wang, C. and Gao, Y. 2019. A new permittivity measurement method for walls in indoor scenes. IEEE Transactions on Antennas and Propagation, 67(4): 2118-2129.

Sivakumar, R., Lee, Y., Azemi, S.N., Ahmad, Z., Soh, P. and You, K. 2022. A Free Space Material Measurement System for Microwave Materials at Kuband. In 2022 IEEE International RF and Microwave Conference (RFM), 19th – 21st, December 2022, Kuala Lumpur, Malaysia: 1-4.

Stavrou, S. and Saunders, SR. 2003, March. Review of constitutive parameters of building materials. In Twelfth International Conference on Antennas and Propagation, 2003 (ICAP 2003). (Conf. Publ. No. 491), 31st March to 3rd April, 2003, Exeter, UK: 211-215.

Vilovic, I., Nad, R., Sipus, Z. and Burum, N. 2008, September. A non-destructive approach for extracting the complex dielectric constant of the walls in building. In 2008 50th ELMAR International Symposium, 10th to 12th September 2008, Zadar, Croatia, (2): 609-612.

Zhang, Y. and Lim, SY. 2020. An investigation into the diffraction effects of building façade for propagation modelling. Progress in Electromagnetics Research, 97: 25-34.

Zhekov, SS., Nazneen, Z., Franek, O. and Pedersen, GF. 2018. Measurement of attenuation by building structures in cellular network bands. IEEE Antennas and Wireless Propagation Letters, 17(12): 2260-2263.

Corresponding author's e-mail address: gbengailori@unilag.edu.ng